INTERNATIONAL JOURNAL FOR NUMERICAL METHODS IN FLUIDS, VOL. 21, 857–867 (1995)

A NUMERICAL STUDY OF VORTEX SHEDDING AROUND A HEATED/COOLED CIRCULAR CYLINDER BY THE THREE-STEP TAYLOR–GALERKIN METHOD

KATSUMORI HATANAKA

Department of Civil Engineering, Nihon University, Narashinodai 7-24-1, Funabashi, Chiba 274, Japan

AND

MUTSUTO KAWAHARA

Department of Civil Engineering, Chuo University, Kasuga 1-13-27, Bunkyoku, Tokyo 112, Japan

SUMMARY

In this paper the vortex shedding around a heated/cooled circular cylinder is numerically simulated by solving the time-dependent Navier–Stokes and energy equations. A finite element method that is referred to as the three-step Taylor–Galerkin method is used to compute these equations. The attention of this study is directed to the investigation of the effect of buoyancy on the vortex street behind the cylinder at constant Reynolds number. The present paper shows the suppression or generation of the von Kármán vortex street behind the cylinder when the cylinder surface is heated or cooled respectively. The relationship between the temperature-induced buoyancy force and the vortex shedding is also discussed through several numerical examples.

KEY WORDS: Taylor–Galerkin method; vortex shedding; buoyancy force; von Kármán vortex street

INTRODUCTION

The vortex shedding around a cylinder and the von Kármán vortex street behind a cylinder have received much attention by many researchers in both experimental and numerical fluid dynamics. The vortex shedding around a circular cylinder is a well-known benchmark problem for the numerical simulation of unsteady, incompressible viscous fluid flow. Successful simulations have been reported by numerous authors using a wide range of numerical methods. However, the problem of vortex shedding for mixed natural and forced convection has not been investigated sufficiently. In the mixed convection regime the flow situation is physically complex or complicated owing to the temperature-induced buoyancy forces added to the viscous phenomena. In this area Noto and Matsumoto[1] first numerically investigated the degeneration of the von Kármán vortex street by a finite difference scheme in the case where the cylinder surface is heated. Jain and Lohar[2] and Noto and Matsumoto[3] have also studied the increase in the vortex-shedding frequency with increasing cylinder temperature. Chang and Sa[4] have reported a detailed study on the vortex mechanisms in the near wake of a heated/cooled circular cylinder by a finite difference scheme. According to their results, cooling of the cylinder surface promotes the generation of the von Kármán vortex street even when the Reynolds number is low; steady twin vortices are usually observed. On the other hand, when the cylinder surface is heated, the suppression of the von Kármán vortex street occurs at relatively high Reynolds numbers. The above investigations, however, were not aimed at studying the flow behaviour around a critical

CCC 0271–2091/95/100857–11

Received 4 June 1994
Revised 28 November 1995

value of the Grashof (or Richardson) number in detail, where the flow suddenly changes from a periodic flow into a steady flow and vice versa.

This paper presents a finite element analysis of the vortex shedding around a heated/cooled circular cylinder, particularly the numerical analysis of the transient flow behaviour around the critical value of the Grashof (or Richardson) number in order to understand the relationship between the buoyancy effect and the vortex shedding in the mixed convection regime. The finite element scheme used in this paper is the three-step Taylor– Galerkin/velocity correction method which has been proposed by us for the numerical simulation of convection-dominated flow problems. We also wish to show the applicability of this method to the numerical simulation of the flow problems mentioned above through numerical examples.

GOVERNING EQUATIONS AND NUMERICAL METHODS

Assuming that the fluid under consideration is an incompressible viscous fluid and the flow is unsteady, the governing equations for the vortex shedding around a heated/cooled circular cylinder can be the Bousinessq-approximated Navier–Stokes equations, the equation of continuity and the energy equation. The non-dimensional forms of these are

$$\frac{\partial u_i}{\partial t} = u_j u_{i,j} + p_{,i} - \frac{1}{Re}(u_{i,j} + u_{j,i})_{,j} - \frac{Gr}{Re^2} f_i T = 0 \quad \text{in} \quad \Omega, \tag{1}$$

$$u_{i,i} = 0 \quad \text{in} \quad \Omega, \tag{2}$$

$$\frac{\partial T}{\partial t} + u_j T_{,j} - \frac{1}{Pe} T_{,jj} = 0 \quad \text{in} \quad \Omega, \tag{3}$$

where u_i is the velocity vector, p is the pressure, T is the temperature, f_i is a unit vector representing the gravitational direction, Re is the Reynolds number, Gr is the Grashof number and Pe is the Peclet number. Ω is the computational domain which is surrounded by the piecewise smooth boundary Γ. The definitions of the non-dimensional parameters are

$$Re = \frac{U_\infty D}{\nu}, \qquad Gr = \frac{\beta g \Delta T D^3}{\nu^2}, \qquad Pe = \frac{U_\infty D}{\alpha}, \tag{4}$$

where U_∞ is the characteristic velocity, D is the characteristic length representing the diameter of the cylinder, ν is the kinematic viscosity, β is the coefficient of volumetric thermal expansion, g is the gravitational acceleration, α is the thermal diffusivity and $\Delta T (= T_c - T_\infty)$ is the temperature difference between a constant cylinder surface temperature T_c and a constant inflow temperature T_∞ (Figure 1). The general boundary conditions for this system are

$$u_i = \hat{u}_i \quad \text{on} \quad \Gamma_1, \tag{5}$$

$$t_i = [-p\delta_{ij} + Re^{-1}(u_{i,j} + u_{j,i}) \cdot n_j = \hat{t}_i \quad \text{on} \quad \Gamma_2, \tag{6}$$

$$T = \hat{T} \quad \text{on} \quad \Gamma_3, \tag{7}$$

$$q = T_{,i} n_i = \hat{T}_{,i} n_i \quad \text{on} \quad \Gamma_4, \tag{8}$$

where δ_{ij} is Kronecker's delta function, n_i are the direction cosines with respect to a set of axes and the superposed hat denotes a function given on the boundaries.

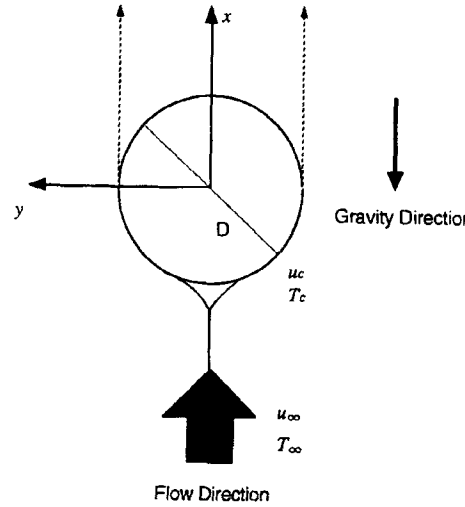

Figure 1. Sketch of vortex-shedding problem around circular cylinder in mixed convection

The initial conditions are

$$u_i(x_i,\ 0) = u_i^{(0)}(x_i), \tag{9}$$

$$T(x_i,\ 0) = T^{(0)}(x_i), \tag{10}$$

where the initial velocity $u_i^{(0)}(x_i)$ satisfies the incompressibility condition.

In order to discretize the governing equations, the three-step Taylor–Galerkin method is successfully used. Let u_i^n and T^n be the known variables of the velocity and temperature fields respectively at time $t^n = t^{n-1} + \Delta t$ $(n = 1,\ 2,\ \ldots)$, where Δt is the time increment. Then the governing equations (1)–(3) can be discretized in time by the forward Euler finite difference scheme

$$\frac{u_i^{n+1} - u_i^n}{\Delta t} + u_j^n u_{i,j}^n + p_{,i}^{n+1} - \frac{1}{Re}(u_{i,j}^n + u_{j,i}^n)_{,j} - \frac{Gr}{Re^2} f_i T^n = 0, \tag{11}$$

$$u_{i,i}^{n+1} = 0, \tag{12}$$

$$\frac{T^{n+1} - T^n}{\Delta t} + u_j^n T_{,j}^n - \frac{1}{Pe} T_{,jj}^n = 0. \tag{13}$$

After taking divergence from both sides of (11) and substituting (12), the pressure Poisson equation can be derived as

$$P_{,ii}^{n+1} = \frac{1}{\Delta t} u_{i,i}^n - u_{j,i}^n u_{i,j}^n - u_j^n u_{i,ij}^n + Re^{-1}(u_{i,j}^n + u_{j,i}^n)_{,ij} + Gr\, Re^{-2}(T^n f_i)_{,i}. \tag{14}$$

The boundary conditions for this are

$$p^{n+1} = \hat{p} \quad \text{on} \quad \Gamma_2, \tag{15}$$

$$p_i^{n+1} n_i = \hat{\gamma}_i \quad \text{on} \quad \Gamma_1. \tag{16}$$

The proper treatment of the boundary conditions for pressure in numerical computations by the velocity correction finite element method has been investigated by us previously.[5]

Once the pressure field has been determined from (14), the velocities u_i^{n+1} can be computed from the discrete momentum equation (11), which can be treated as a convection–diffusion equation.

Many solution techniques for the convection–diffusion type of equation have been proposed in the last few decades. The Taylor–Galerkin method is one of the Lax–Wendroff methods and was first proposed by Donea and co-workers[6,7] in the finite element method for computing convection-dominated flow fields. They concluded that in this context the Taylor–Galerkin method has third-order accuracy in space and time and good stability within a certain Courant number range ($Cr \leq 1{\cdot}0$). The use of the Taylor–Galerkin method does not require the specification of a proper parameter value for the stability of the computation, which is sometimes required in other methods such as upwinding methods, higher-order methods and so on (see e.g. References 8–10). However, the Taylor–Galerkin method includes the third-derivative term in the discretized momentum equations, which is undesirable for linear interpolation functions. We have therefore proposed the three-step Taylor–Galerkin method for the numerical simulation of convection-dominated flows with linear interpolation functions in the spatial and temporal discretizations. One of the ideas of the present time-stepping algorithm has come from the two-step Lax–Wendroff finite element method proposed by Kawahara.[11] In this method we express the time derivative terms of the Taylor series of an objective variable up to the second-derivative term by analogy with the manner of the second-order Runge–Kutta scheme. Details of this method can be found in References 12 and 13.

In accordance with the discretization manner of the present method, the discretized momentum, energy and pressure Poisson equations (11), (13) and (14) can be rewritten in three time integration steps as follows:

step 1

$$u_i^{n+1/3} = u_i^n - \frac{\Delta t}{3}\left(u_j^n u_{i,j}^n + p_{,i}^n - \frac{1}{Re}(u_{i,j}^n + u_{j,i}^n)_{,j} - \frac{Gr}{Re^2} f_i T^n\right), \tag{17}$$

$$T^{n+1/3} = T^n - \frac{\Delta t}{3}\left(u_j^n T_{,j}^n - \frac{1}{Pe} T_{,jj}^n\right), \tag{18}$$

step 2

$$u_i^{n+2/3} = u_i^n - \frac{\Delta t}{2}\left(u_j^{n+1/3} u_{i,j}^{n+1/3} + p_{,i}^n - \frac{1}{Re}(u_{i,j}^{n+1/3} + u_{j,i}^{n+1/3})_{,j} - \frac{Gr}{Re^2} f_i T^{n+1/3}\right), \tag{19}$$

$$T^{n+2/3} = T^n - \frac{\Delta t}{2}\left(u_j^{n+1/3} T_{,j}^{n+1/3} - \frac{1}{Pe} T_{,jj}^{n+1/3}\right), \tag{20}$$

step 3

$$p_{,ii}^{n+1} = \frac{1}{\Delta t} u_{i,i}^n - u_{j,i}^{n+2/3} u_{i,j}^{n+2/3} - u_j^{n+2/3} u_{i,ij}^{n+2/3} + \frac{1}{Re}(u_{i,j}^{n+2/3} + u_{j,i}^{n+2/3})_{,ij} + \frac{Gr}{Re^2}(T^{n+2/3} f_i)_{,i}, \tag{21}$$

$$u_i^{n+1} = u_i^n - \Delta t\left(u_j^{n+2/3} u_{i,j}^{n+2/3} + p_{,i}^{n+1} - \frac{1}{Re}(u_{i,j}^{n+2/3} + u_{j,i}^{n+2/3})_{,j} - \frac{Gr}{Re^2} f_i T^{n+2/3}\right), \tag{22}$$

$$T^{n+1} = T^n - \Delta t\left(u_j^{n+2/3} T_{,j}^{n+2/3} - \frac{1}{Pe} T_{,jj}^{n+2/3}\right). \tag{23}$$

In these equations $u_i^{n+1/3}$, $u_i^{n+2/3}$, $T^{n+1/3}$ and $T^{n+2/3}$ stand for the intermediate velocity and temperature variables which complete the third-derivative terms in the Taylor series for the unknown velocity and temperature variables u_i^{n+1} and T^{n+1}.

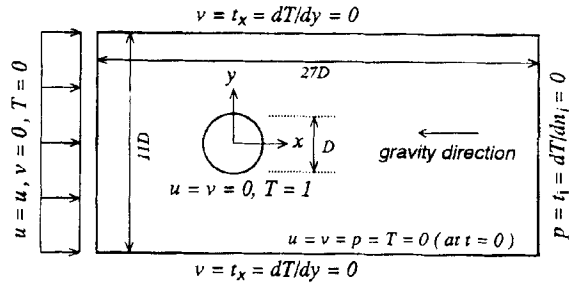

Figure 2. Analytical domain and boundary conditions

The use of the standard Galerkin method with linear triangular finite elements can yield the finite element formulations of (17)–(23). A stability analysis of the present method has been performed by us[13] and it has been confirmed that the present method has third-order accuracy and good stability for the numerical simulation of the unsteady one-dimensional pure advection equation.

NUMERICAL RESULTS AND DISCUSSION

Numerical simulations of the vortex shedding around a heated/cooled circular cylinder have been examined in the Grashof number range $-10{,}000 \leq Gr \leq 10{,}000$. The constant Reynolds number was selected as $Re = 100$, making the Richardson number

$$Ri = \frac{Gr}{Re^2} \tag{24}$$

in the range $-1{\cdot}0 \leq Ri \leq 1{\cdot}0$. The Prandtl number Pr $(= \nu/\alpha)$ is selected to be 0·706, which yields a Peclet number Pe $(= Pr\ Re)$ of 70·6.

The computational domain and the boundary conditions used in this computation are illustrated in Figure 2. The outflow domain was taken to be a distance of 21·5 units downstream from the cylinder centre. The inlet temperature T_∞ is specified as $T = 0$ and the cylinder surface temperature T_c is taken to be $T = 1{\cdot}0$. The heated/cooled cylinder surface situation was expressed by the direction of the effect of buoyancy forces. The heated cylinder surface was represented by a positive Richardson number, showing that the buoyancy effect works in the opposite direction to the gravitational force, and the cooled cylinder surface was represented by a negative Richardson number. $Ri = 0{\cdot}0$ expresses the non-heated situation in which the vortex shedding is not influenced by the buoyancy force at all. Figure 3 shows the finite element mesh used in this simulation. The total numbers of nodes and elements are 1964 and 3744 respectively.

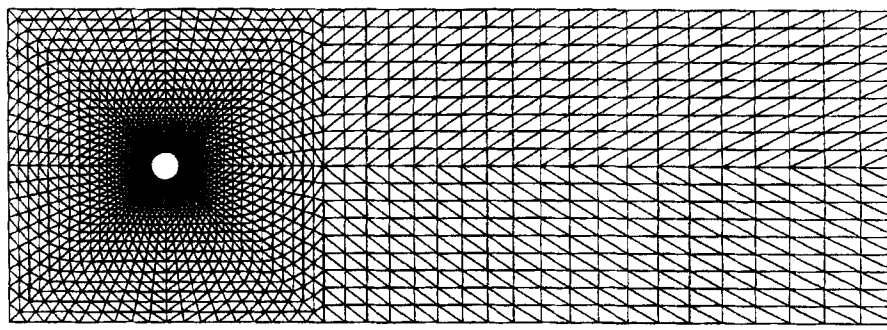

Figure 3. Finite element mesh (1964 nodes and 3744 elements)

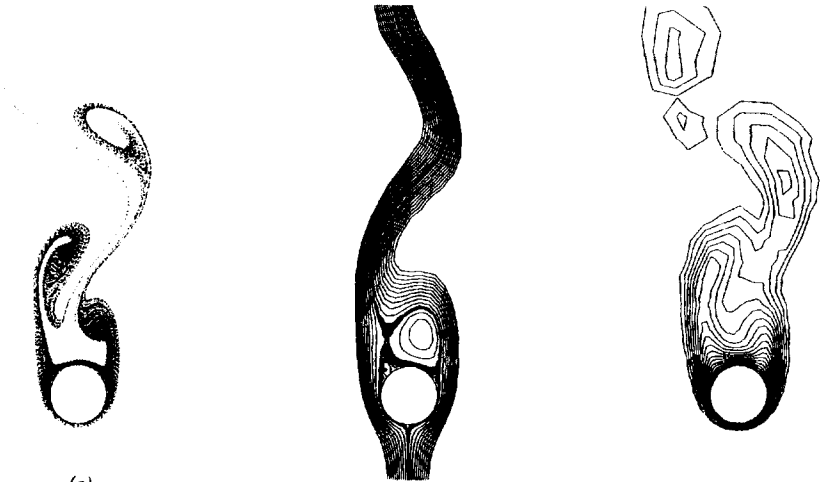

Figure 4. Numerical results of vortex shedding around non-heated cylinder surface at $Re = 100$ ($Ri = 0{\cdot}0$)

The numerical results for $Ri = -1{\cdot}0$, $-0{\cdot}5$, $0{\cdot}0$, $0{\cdot}5$ and $1{\cdot}0$ are shown in Figures 4–8. Upon increasing the Richardson number from $Ri = 0{\cdot}0$ (Figure 4) to $1{\cdot}0$, the periodic von Kármán vortex street behind the cylinder disappeared and the flow became steady with twin vortices just behind the cylinder (Figures 5 and 6). In contrast, the von Kármán vortex street was enhanced upon decreasing the Richardson number (Figures 7 and 8). The computed Strouhal number versus the Richardson number is illustrated in Figure 9 and indicates that the breakdown of the Kármán vortex street occurs near $Ri = 0{\cdot}15$. This sudden vanishing of vortices has also been observed experimentally by Noto and Matsumoto[3] and in other numerical computations (see e.g. Reference 4) at the same Richardson number. A probable reason for the flow behaviour observed in this computation is that the separation points on both sides of the cylinder surface were moved downstream by the buoyancy force as the

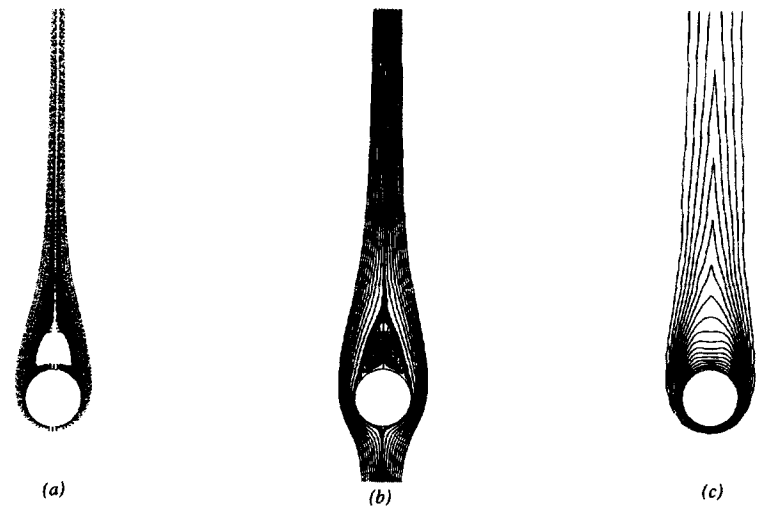

Figure 5. Numerical results of vortex shedding around heated cylinder surface at $Re = 100$ ($Ri = 0{\cdot}5$): (a) streaklines; (b) streamlines; (c) isotherms

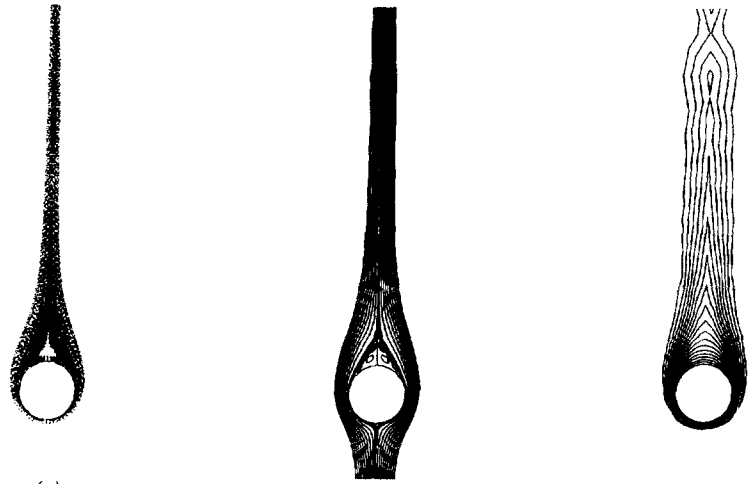

Figure 6. Numerical results of vortex shedding around heated cylinder surface at $Re = 100$ ($Ri = 1{\cdot}0$): (a) streaklines; (b) streamlines; (c) isotherms

Richardson number increased (as one can see in Figure 10). The movement of the separation points downstream may increase the interactions of the vortices; then the breakdown of the von Kármán vortex street occurs and the subsequent flow becomes steady. In order to observe the above phenomena in detail, computations with Richardson numbers in the range $0{\cdot}0 \leq Ri \leq 0{\cdot}15$ have been performed using the present method. The streaklines of the numerical results at a dimensionless time of 150 are shown in Figure 11. According to these results, the breakdown of the von Kármán vortex street occurs at $Ri = 0{\cdot}125$ (Figure 11(b)) and the flow becomes steady state at $Ri = 0{\cdot}15$ (Figure 11(c)). After Ri exceeds 0·12, the stationary twin vortices attach to the cylinder surface and the flow becomes symmetrical with respect to the x-axis.

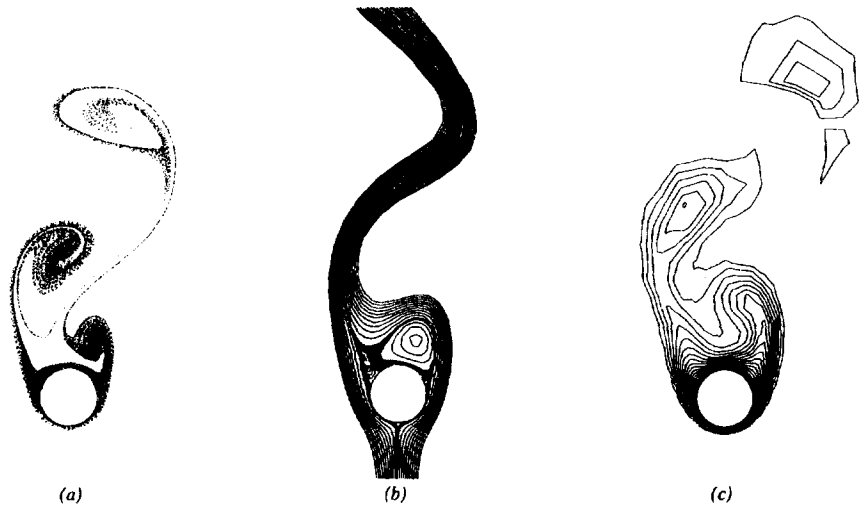

Figure 7. Numerical results of vortex shedding around cooled cylinder surface at $Re = 100$ ($Ri = -0{\cdot}5$): (a) streaklines; (b) streamlines; (c) isotherms

Figure 8. Numerical results of vortex shedding around cooled cylinder surface at $Re = 100$ ($Ri = -1.0$): (a) streaklines; (b) streamlines; (c) isotherms

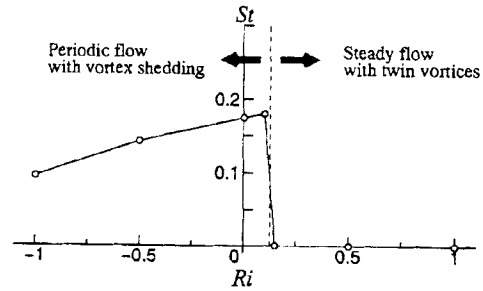

Figure 9. Strouhal number versus Richardson number

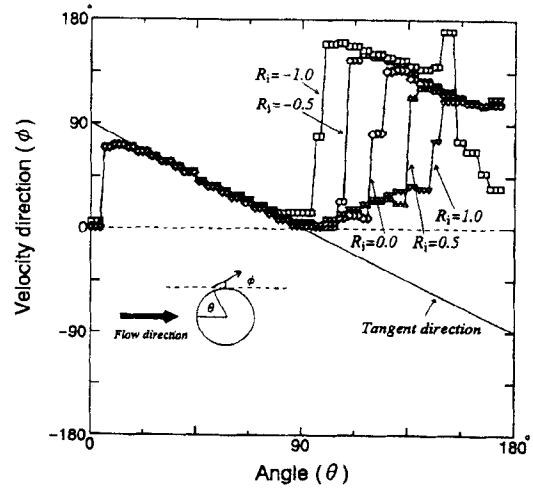

Figure 10. Velocity direction on cylinder surface

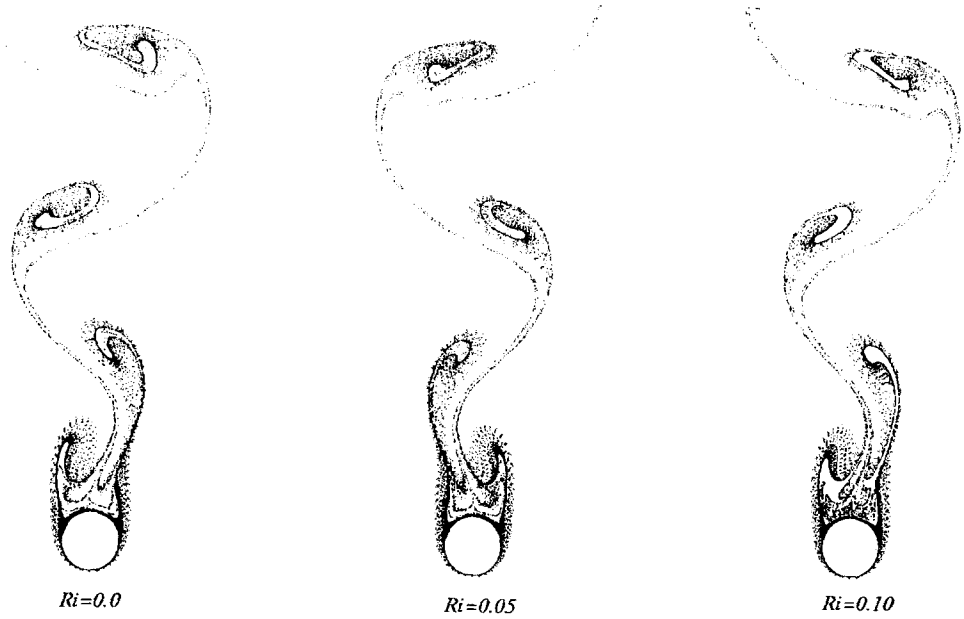

Figure 11(a). Streaklines behind cylinder at $t = 150$ ($Re = 100$)

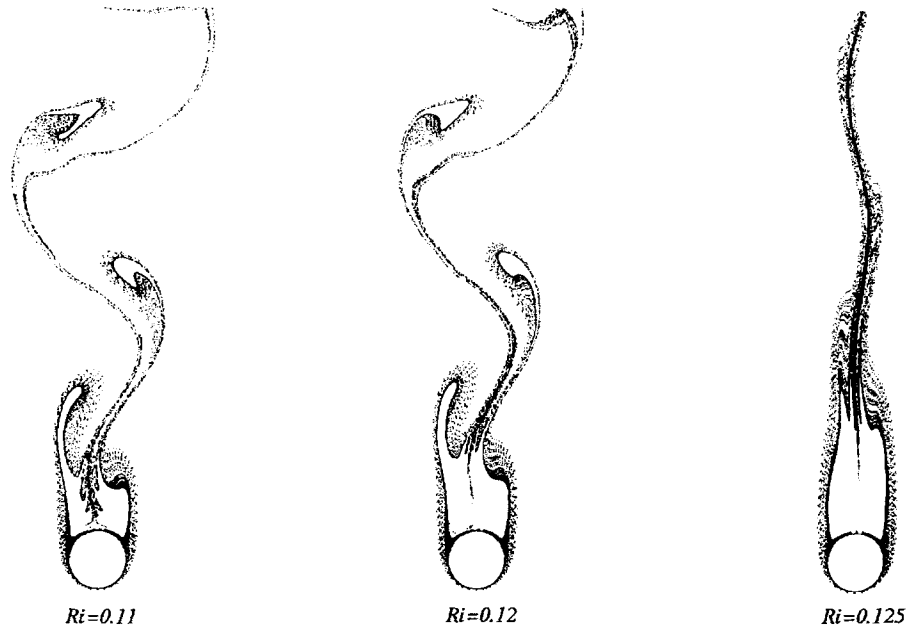

Figure 11(b). Streaklines behind cylinder at $t = 150$ ($Re = 100$)

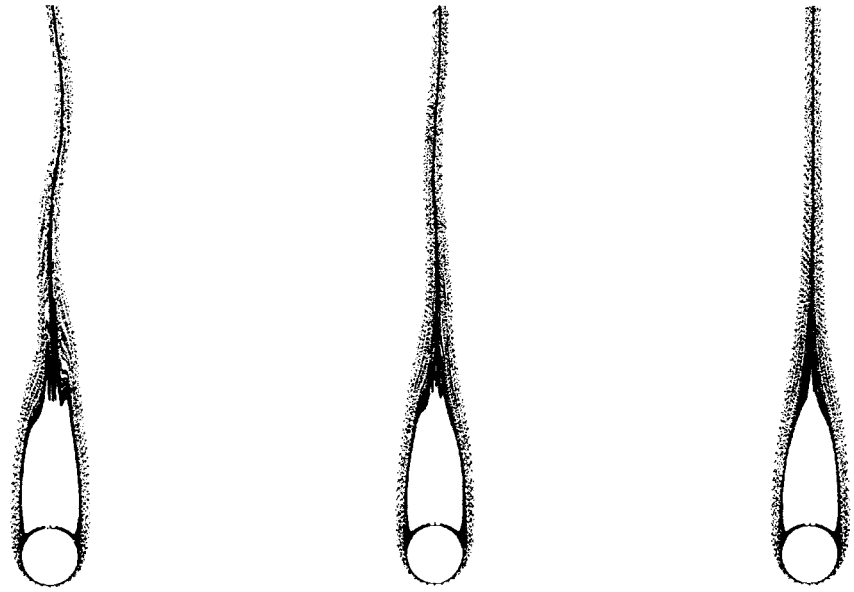

Figure 11(c). Streaklines behind cylinder at $t = 150$ ($Re = 100$)

CONCLUSIONS

The vortex shedding around a heated/cooled circular cylinder has been simulated by the three-step Taylor–Galerkin/velocity correction method. The numerical results provided herein show the interesting behaviour of the flow around the cylinder in the mixed convection regime. The following remarks on the present simulation can be made.

1. As the Richardson number increases, the vortex-shedding frequency is increased owing to the positive buoyancy force. The von Kármán vortex shedding disappears at approximately $Ri = 0{\cdot}15$. The flow patterns eventually become steady with symmetric twin vortices.
2. When the cylinder surface is cooled, the vortex-shedding frequency is decreased. However, the asymmetric flow pattern behind the cylinder is enhanced owing to the negative buoyancy force. The von Kármán vortex street behind the cylinder is consequently enlarged.

The role of the Reynolds number in these phenomena, three-dimensional simulations and simulations of the compressible flow in the mixed convection regime will be the subjects of future study.

REFERENCES

1. K. Noto and R. Matsumoto, 'Numerical simulation on development of the Kármán vortex street due to the negative buoyancy force', *Numer. Methods Lamin. Turbul. Flow*, **5**, 796 (1987).
2. P. C. Jain and B. L. Lohar, 'Unsteady mixed convection heat transfer from a horizontal circular cylinder', *J. Heat Transfer*, **98**, 303 (1979).
3. K. Noto and R. Matsumoto, 'Generation and suppression of the Kármán vortex street upon controlling surface temperature of a cylinder', *Numer. Methods Lamin. Turbul. Flow*, **7**, 671 (1991).
4. K. S. Chang and J. Y. Sa, 'The effect of buoyancy on vortex shedding in the near wake of a circular cylinder', *J. Fluid Mech.*, **220**, 253 (1990).

5. K. Hatanaka and M. Kawahara, 'A fractional step finite element method for conductive–convective heat transfer problem', *Int. J. Numer. Methods Heat Fluid Flow*, **1**, 77 (1991).
6. V. Selmin, J. Donea and L. Quartapelle, 'Finite element methods for nonlinear advection', *Comput. Methods Appl. Mech. Eng.*, **52**, 817–845 (1985).
7. J. Donea, S. Giuliani and L. Quartapelle, 'Time-accurate solution of advection–diffusion problems', *J. Comput. Phys.*, **70**, 463– 499 (1987).
8. A. N. Brooks and T. J. R. Hughes, 'Streamline upwind/Petrov–Galerkin formulations for convection dominated flows with particular emphasis on the incompressible Navier–Stokes equations', *Comput. Methods Appl. Mech. Eng.*, **32**, 199 (1982).
9. M. Kawahara and H. Hirano, 'Two step explicit finite element method for high Reynolds number viscous fluid flow', *Proc. JSCE*, **329** (1983).
10. M. Kawahara, H. Hirano and T. Kodama, 'Two-step explicit finite element method for high Reynolds number flow passed through oscillating body', *Finite Elem. Fluids*, **5**, 227 (1984).
11. M. Kawahara, 'Convergence of finite element Lax–Wendroff method for linear hyperbolic differential equation', *Proc. JSCE*, **253**, 95 (1976).
12. C. B. Jiang and M. Kawahara, 'The analysis of unsteady incompressible flows by a three-step finite element method', *Int. j. numer. methods fluids*, **16**, 793 (1993).
13. C. B. Jiang, K. Hatanaka, M. Kawahara and K. Kashiyama, 'A three-step finite element method for convection dominated incompressible flow', *Comput. Fluid Dyn. J.*, **1**, 447 (1993).
14. K. Noto and R. Matsumoto, 'A breakdown of the Kármán vortex street due to the natural convection', *Flow Visual.*, **III**, 348 (1985).